eNeuro

*Research Article: New Research | Disorders of the Nervous System*

# Cocaine Exposure Modulates Perineuronal Nets and Synaptic Excitability of Fast-spiking Interneurons in the Medial Prefrontal Cortex

**Megan L. Slaker[1], Emily T. Jorgensen[3], Deborah M. Hegarty[2], Xinyue Liu[4], Yan Kong[4], Fuming Zhang[4], Robert J. Linhardt[4], Travis E. Brown[3], Sue A. Aicher[2] and Barbara A. Sorg[1]**

[1]*Department of Integrative Physiology and Neuroscience, Translational Addiction Research Center, Washington State University, Vancouver, Washington 98686, USA*

[2]*Department of Physiology and Pharmacology, Oregon Health & Science University, Portland, Oregon 97239, USA*

[3]*School of Pharmacy and Department of Neuroscience, University of Wyoming, Laramie, Wyoming 82071, USA*

[4]*Department of Chemistry and Chemical Biology, Center for Biotechnology and Interdisciplinary Studies, Rensselaer Polytechnic Institute, Troy, New York, 12180, USA*

DOI: 10.1523/ENEURO.0221-18.2018

Received: 4 June 2018

Revised: 6 September 2018

Accepted: 13 September 2018

Published: 1 October 2018

**Author contributions:** BAS designed and interpreted the behavioral data and immunohistochemical data for PV and PNN intensity analysis, wrote and revised the manuscript; MLK performed the behavioral components and immunohistochemical analysis for the PV and PNN intensity analysis and wrote the manuscript; DMH performed the immunohistochemistry and Imaris analysis of puncta data and revised the manuscript; SAA designed, analyzed and interpreted the puncta study and revised the manuscript; XL and YK performed the LC-MS analysis, FZ and RJL designed the GAG analysis experiments and helped in writing the manuscript; TEB helped to design and interpret the electrophysiological data and wrote and revised portions of the manuscript, and ETJ performed the electrophysiological experiments and wrote portions of the manuscript.

**Funding:** http://doi.org/10.13039/100000026HHS | NIH | National Institute on Drug Abuse (NIDA)
033404
040965
040965

**Funding:** http://doi.org/10.13039/100000057HHS | NIH | National Institute of General Medical Sciences (NIGMS)
103398

**Funding:** http://doi.org/10.13039/100000065HHS | NIH | National Institute of Neurological Disorders and Stroke (NINDS)
061800

**Funding:** http://doi.org/10.13039/100000062HHS | NIH | National Institute of Diabetes and Digestive and Kidney Diseases (NIDDK)
111958

**Funding:** http://doi.org/10.13039/100000050HHS | NIH | National Heart, Lung, and Blood Institute (NHLBI)
125371

**Conflict of Interest:** Author reports no conflict of interest.

***Correspondence:*** Barbara A. Sorg, Department of Integrative Physiology and Neuroscience, Washington State University, Vancouver, WA 98686, USA. PH: 360-546-9719; FX: 360-546-9038; E-mail: barbsorg@wsu.edu

**Cite as:** eNeuro 2018; 10.1523/ENEURO.0221-18.2018

# Cocaine Exposure Modulates Perineuronal Nets and Synaptic Excitability of Fast-spiking Interneurons in the Medial Prefrontal Cortex

Megan L. Slaker[1], Emily T. Jorgensen[3], Deborah M. Hegarty[2], Xinyue Liu[4], Yan Kong[4], Fuming Zhang[4], Robert J. Linhardt[4], Travis E. Brown[3], Sue A. Aicher[2], Barbara A. Sorg[1]

[1]Department of Integrative Physiology and Neuroscience, Translational Addiction Research Center, Washington State University, Vancouver, Washington 98686, [2]Department of Physiology and Pharmacology, Oregon Health & Science University, Portland, Oregon 97239, [3]School of Pharmacy and Department of Neuroscience, University of Wyoming, Laramie, Wyoming 82071, [4]Department of Chemistry and Chemical Biology, Center for Biotechnology and Interdisciplinary Studies, Rensselaer Polytechnic Institute, Troy, New York, 12180

*Correspondence:*

Barbara A. Sorg
Department of Integrative Physiology and Neuroscience
Washington State University
Vancouver, WA 98686
PH: 360-546-9719
FX: 360-546-9038
barbsorg@wsu.edu

*Abbreviated Title:* Impact of cocaine on prefrontal cortex parvalbumin cells

Number of pages: 29
Number of Figures: 5
Number of Tables: 2
Extended Data: 1

**Abstract**

We previously reported that perineuronal nets (PNNs) are required for cocaine-associated memories. Perineuronal nets are extracellular matrix that primarily surrounds parvalbumin (PV)-containing, GABAergic fast-spiking interneurons (FSIs) in the medial prefrontal cortex (mPFC). Here we measured the impact of acute (1 day) or repeated (5 days) cocaine exposure on PNNs and PV cells within the prelimbic and infralimbic regions of the mPFC. Adult rats were exposed to 1 day or 5 days of cocaine and stained for PNNs (using *Wisteria floribunda* agglutinin, WFA) and PV intensity 2 h or 24 h later. In the prelimbic and infralimbic PFC, PNN staining intensity decreased 2 hr after 1 day of cocaine but increased after 5 days of cocaine. Cocaine also produced changes in PV intensity, which generally lagged behind that of PNNs. In the prelimbic PFC, both 1 and 5 days of cocaine increased GAD65/67 puncta near PNN-surrounded PV cells, with an increase in the ratio of GAD65/67:VGluT1 puncta after 5 days of cocaine exposure. In the prelimbic PFC, slice electrophysiology studies in FSIs surrounded by PNNs revealed that both 1 and 5 days of cocaine reduced the number of action potentials 2 h later. Synaptic changes demonstrated that 5 d cocaine increased inhibition of FSIs, potentially reducing the inhibition of pyramidal neurons and contributing to their hyperexcitability during relapse behavior. These early and rapid responses to cocaine may alter network stability of PV FSIs that partially mediate the persistent and chronic nature of drug addiction.

**Significance Statement**

Parvalbumin-containing, FSIs control the inhibitory:excitatory balance in the adult CNS, and the majority of these are surrounded by PNNs. The mPFC is critical to relapse in cocaine addiction, yet few studies have focused on the impact of cocaine exposure on PV interneurons that profoundly control output of the mPFC. Our studies highlight the impact of cocaine on PV and PNN levels and intrinsic and synaptic properties of PNN-surrounded FSIs in the mPFC. These findings point to a key upstream mechanism by which FSIs may contribute to the consistently observed increase in mPFC excitatory output of pyramidal neurons that contribute to cocaine reinstatement, and they have broader implications for understanding how PNN-surrounded neurons may control aberrant learning processes involved in addiction.

## Introduction

Pyramidal neurons in the medial prefrontal cortex (mPFC) that project to the nucleus accumbens control cocaine-seeking behavior in rodent models of addiction (McFarland and Kalivas, 2001; McLaughlin and See, 2003; McFarland et al., 2004; Ma et al., 2014). However, surprisingly few studies (Kroener and Lavin, 2010; Campanac and Hoffman, 2013) have examined the impact of cocaine on fast-spiking, GABAergic interneurons, which contain parvalbumin (PV) (Kawaguchi and Kubota, 1993). PV neurons profoundly control the output of these mPFC pyramidal neurons, and in the mPFC, PV FSIs contain D1 and D2 dopamine receptors (LeMoine and Gaspar, 1998) and synapse directly onto layer V pyramidal neurons to control their output (Lee et al., 2014).

Approximately 60-80% of PV cells in the cortex are enwrapped by perineuronal nets (PNNs) (Bruckner et al., 1993; Slaker et al., 2015), which are aggregations of extracellular matrix (ECM) molecules that appear during development in an experience-dependent manner. Maturation of PV cells with PNNs coincides with the closure of developmental critical periods and PV network stabilization (Pizzorusso et al., 2002; Balmer et al., 2009; Gogolla et al., 2009; Kwok et al., 2011). Several studies have demonstrated an important contribution of PNNs to learning and memory (Balmer et al., 2009; Fawcett, 2009; Gogolla et al., 2009; Romberg et al., 2013; Banerjee et al., 2017; Foscarin et al., 2017). We previously found that the consolidation and reconsolidation of cocaine-associated memories were dependent on intact PNNs in the mPFC (Slaker et al., 2015), and others have reported a role for PNNs in drug-related behaviors (Van den Oever et al., 2010b; Xue et al., 2014; Vazquez-Sanroman et al., 2015b).

The findings that removal of PNNs alters learning and memory strongly suggest that PNNs themselves may be a target for stimuli that induce learning and memory, including drugs of abuse. Even during adulthood, PNNs are dynamic structures modulated by experience that changes the intensity of PNN staining. For example, exposure to environmental enrichment in rodents decreases the intensity of PNN staining within the somatosensory cortex, motor cortex, and cerebellum (Foscarin et al., 2011; Madinier et al., 2014). The intensity of PNNs (as labeled by *Wisteria floribunda* agglutinin (WFA)) is commonly used as an indirect measure of their developmental maturity, with dim staining representing an immature PNN and bright staining representing a mature PNN (Foscarin et al., 2011; Wang and Fawcett, 2012). Dynamic changes in PV intensity also occur after learning and memory, and are associated with changes in PV

network activity that powerfully controls output of neurons embedded within the network (Donato et al., 2013; Favuzzi et al., 2017)

Here we defined the early impacts of acute (1 day) and repeated (5 days) cocaine on dynamic changes on the intensity of PNNs and PV and on the electrical signaling in PNN-surrounded FSIs in the mPFC of adult rats. Early changes in these neurons may well contribute to the cocaine-induced hyperexcitability of mPFC pyramidal neurons reported by us and several others (Dong et al., 2005; Nasif et al., 2005; Huang et al., 2007; Hearing et al., 2013; Slaker et al., 2015), which promotes reinstatement behavior. In the current study, we determined the extent to which acute and repeated cocaine exposure altered the intensity of PNNs and PV as well as functional changes in FSIs surrounded by PNNs. We found that acute cocaine exposure decreased PNNs and PV intensity, while repeated cocaine increased PNNs and PV intensity in the prelimbic PFC, suggesting that acute cocaine exposure shifted PV cells to a less mature state, while repeated cocaine shifted these cells to a more mature state. Repeated cocaine exposure decreased the excitability of PV FSIs, consistent with an increase in the inhibitory:excitatory ratio of puncta on these cells, and it increased mini inhibitory postsynaptic potential (mIPSC) frequency and amplitude. Altogether, these changes may significantly contribute to the hyperexcitability of pyramidal neurons in the prelimbic PFC that contribute to drug reinstatement.

## Materials and Methods

### *Animals*

Adult male Sprague Dawley rats obtained from Simonsen Laboratories (Gilroy, CA) were used in these studies. A total of 127 rats were used (56 for WFA/PV intensity analyses (a subset of 16 rats was used for puncta analysis); 16 for CSPG analyses, and 55 for electrophysiological recordings (29 for intrinsic recordings and 26 for synaptic recordings). Rats weighed 330.1 ± 2.5 g (mean ± SEM) at the start of each experiment. All animals were singly housed in a temperature- and humidity-controlled room with a 12 h light/dark cycle in which lights were on at 7:00 am or 7:00 pm. Previous work has demonstrated no changes in early cocaine sensitization at these times (Sleipness et al., 2005). Food and water were available *ad libitum* throughout the experiment, except during behavioral testing. All experiments were approved by the Washington State University and the University of Wyoming Institutional Animal Care and Use Committees and according to the National Institutes of Health *Guide for the Care and Use of Laboratory*

*Animals*. All efforts were made to reduce the number of animals and to minimize pain and suffering.

*Drugs*

Cocaine hydrochloride was a gift from the National Institute on Drug Abuse. The cocaine salt was dissolved in sterile saline as weight of the salt to a final concentration of 15 mg/ml. Cocaine and saline were administered intraperitoneal (i.p.) as 1 ml/kg.

*Materials for Chondroitin Sulfate Proteoglycan Analysis*

Unsaturated disaccharide standards of chondroitin sulfate (CS) (ΔUA-GalNAc; ΔUA-GalNAc4S; ΔUA-GalNAc6S; ΔUA2S-GalNAc; ΔUA2S-Gal-NAc4S; ΔUA2S-GalNAc6S; ΔUA-GalNAc4S6S; ΔUA2S-GalNAc4S6S), unsaturated disaccharide standards of HS (ΔUA-GlcNAc; ΔUA-GlcNS; ΔUA-GlcNAc6S; ΔUA2S-GlcNAc; ΔUA2S-GlcNS; ΔUA-GlcNS6S; ΔUA2S-GlcNAc6S; ΔUA2S-GlcNS6S), and unsaturated disaccharide standard of HA (ΔUA-GlcNAc), where ΔUA is 4-deoxy-α-L-*threo*-hex-4-enopyranosyluronic acid, were purchased from Iduron (UK). Actinase E was obtained from Kaken Biochemicals (Japan). Chondroitin lyase ABC from *Proteus vulgaris* was expressed in the laboratory of R.J.L. Recombinant *Flavobacterial* heparin lyases I, II, and III were expressed in the R.J.L. laboratory using *Escherichia coli* strains provided by Jian Liu (College of Pharmacy, University of North Carolina). AMAC and sodium cyanoborohydride ($NaCNBH_3$) were obtained from Sigma-Aldrich (St. Louis, MO, USA). All other chemicals were of HPLC grade. Vivapure Q Mini H strong anion exchange spin columns were from Sartoriou Stedim Biotech (Bohemia, NY, USA).

*Cocaine Exposure*

A three-chamber apparatus (total dimensions: 68 X 21 X 21 cm) was used to assess locomotor activity (Med Associates). Animals were allowed access to the entire apparatus and locomotor activity was recorded automatically with infrared photocell beams.

Rats were gently handled for 5 days before the start of the experiment. On the first day of the experiment, rats were given a 15 min habituation period to the apparatus to limit novelty-induced locomotor effects on future testing days. Rats were assigned to the cocaine or saline group by counterbalancing locomotor activity during the habituation day. On subsequent days, rats were given a dose of saline (1 ml/kg, i.p.) or cocaine (15 mg/kg, i.p.) and immediately placed in the apparatus for 30 min with locomotor activity reported the first 15 min.

*Tissue collection*

For immunohistochemistry, 2 or 24 h following the last injection, rats were perfused intracardially with 4% paraformaldehyde (PFA) in phosphate buffered saline (PBS). The brains were removed and stored overnight in 4% PFA at 4˚C. The following day, brains were moved to a 20% sucrose solution, and 24 h later were frozen with powdered dry ice and stored at -80 ˚C until analysis. For mass spectrometry, 2 h following the last injection, rats were rapidly decapitated and mPFC tissue containing primarily the prelimbic PFC was dissected and flash frozen on dry ice in a microcentrifuge tube. Tissue was stored at -80 ˚C and shipped on dry ice.

*Immunohistochemistry and Imaging*

PV and WFA labeling and imaging These studies were conducted as previously described (Slaker et al., 2016). Anatomical landmarks were used to determine representative caudal and rostral sections of prelimbic cortex that were within bregma approximately +3.2 to +4.2 mm (Paxinos G, 1998). Serial coronal brain sections were cut at 30 µm using a freezing microtome. Sections were maintained in a storage buffer solution until immunohistochemistry was performed. To assess PV and WFA staining, free-floating sections were washed three times for 5 min in PBS and then quenched in 50% ethanol for 30 min. After a set of three 5 min washes in PBS, the sections were placed in 3% goat blocking serum (Vector Laboratories) for 1 h. Tissue was incubated at 4˚C on a rocker overnight with an antibody against PV (Millipore Cat# MAB1572, RRID: AB_2174013, 1:1000) in PBS containing 2% goat serum. After three 10 min washes, tissue was incubated for 2 h with secondary goat anti-mouse AlexaFluor-594 antibody (Thermo Fisher, Cat# R37121, RRID: AB_2556549,1:500). After three 10 min washes in PBS, tissue was incubated for 2 h with fluorescein-conjugated WFA (Vector Laboratories, Cat# FL-1351, RRID: AB_2336875, 1:500). Tissue was washed three more times for 10 min and then mounted on Frost plus slides in diluted PBS with X-100 (0.15 X PBS, 0.24% Triton X-100). Slides were stored flat until dry (at least 24 h) at 4˚C. The slides were coverslipped with ProLong Gold (Life Technologies) and stored flat at 4˚C until time of imaging. Images of the prelimbic and infralimbic PFC were taken using a Leica SP8 laser scanning confocal microscope with Leica Application Suite. An HCX PL apo CS, dry, 20X objective with 0.70 numerical aperture was used for all images. WFA-bound fluorescein was excited using a 488 laser, and a photomultiplier tube detected emission photons within the range of 495 - 545 nm. AlexaFlour 594 was excited using a 561 laser, and a photomultiplier tube detected emission photons within the range of 585 – 645 nm. Images were taken through a z-plane (9 µm) at the center of the tissue containing 20 stacks within each region. Gain, offset, laser intensity, zoom,

and pinhole were kept constant for all images. Sequences of the raw images from the z-stack were exported and projected into a sum slices image using ImageJ software (NIH).

*Quantification and Statistical Analysis*

WFA and PV intensity were quantified using ImageJ software (RRID: SCR_003070) as previously described (Slaker et al., 2016). Briefly, background subtraction from each projection image was conducted by first using the Rolling Ball Radius function and then determining two standard deviations above the mean within a region of the image containing no visible PNNs. Each visible PNN (surrounding at least 2/3 of the underlying cell body) in the image was assigned as a region of interest, including the cell body and proximal dendrites. The average intensity for each region of interest (each PNN) was calculated and recorded. All intensity values were normalized to the average intensity value from the control group (saline) for each region. To assess correlations between WFA and PV staining intensity, raw PV intensity was grouped together based on bins of 10 arbitrary units (AUs) and then within each bin, the corresponding raw intensity of WFA (in AUs) from the same cell was averaged. All measurements were made by an experimenter blinded to the treatment conditions.

Puncta labeling and imaging Immunohistochemical methods were similar to those previously described (Hegarty et al., 2010; Hegarty et al., 2014). Solutions were prepared in either 0.1 M phosphate buffer at pH 7.4 (PB) or 0.1 M Tris-buffered saline at pH 7.6 (TS). Tissue sections were first rinsed in PB, then incubated in 1% sodium borohydride in PB for 30 min to reduce background. After rinses in PB and TS, sections were incubated in 0.5% bovine serum albumin (BSA) in TS for 30 min and then placed in a primary antibody cocktail made in 0.1% BSA and 0.25% Triton X-100 in TS for two nights at 4°C. The primary antibody cocktail consisted of goat anti-glutamic acid decarboxylase 65/67 (GAD 65/67, Santa Cruz Biotechnology, Cat# sc-7513, RRID: AB_2107745, 1:100), rabbit anti-parvalbumin (Novus Biologicals, Cat# NB120-11427, RRID:AB_791498, 1:1000), and guinea pig anti-vesicular glutamate transporter 1 (VGluT1; EMD Millipore, Cat# AB5905, RRID: AB_2301751, 1:5000). After 40 h primary antibody incubation, tissue sections were rinsed in TS and then incubated with a cocktail of fluorescently-labeled secondary antibodies for 2 h, light-protected, at room temperature. The secondary antibody cocktail consisted of Alexa Fluor 488 donkey anti-goat (ThermoFisher Scientific, Cat# A11055, RRID: AB_2534102, 1:800), Alexa Fluor 546 donkey anti-rabbit (ThermoFisher Scientific, Cat# A10040, RRID: AB_2534016, 1:800;); and Alexa Fluor 647 donkey anti-guinea pig (Jackson ImmunoResearch Laboratories, Cat# 706-605-148, RRID: AB_2340476, 1:800).

Tissue sections were rinsed again in TS and then incubated in biotinylated *Wisteria floribunda* lectin (WFA, Vector Laboratories, Cat# B-1355, RRID: AB_2336874, 1:50) for 2 h at room temperature. Following TS rinses, tissue sections were incubated for 3 h at room temperature in Alexa Fluor 405-conjugated streptavidin (ThermoFisher Scientific, Cat# S32351, 6.25 µg / ml). Finally, tissue sections were rinsed in TS followed by PB before being mounted with 0.05 M PB onto gelatin-coated slides to dry. Slides were coverslipped with Prolong Gold Antifade Mountant (ThermoFisher Scientific) and light-protected until imaging.

Anatomical landmarks used were those described above for PV and WFA labeling. To determine representative caudal and rostral sections of prelimbic cortex that were within bregma +3.5 to +4.2 mm (Paxinos G, 1998). Two high magnification images were taken at each level of the prelimbic cortex (2 images/level x 2 levels/animal = 4 images/animal). Images were captured on a Zeiss LSM 780 confocal microscope with a 63 x 1.4 NA Plan-Apochromat objective (Carl Zeiss MicroImaging, Thornwood, NY) using the single pass, multi-tracking format at a 1024 x 1024 pixel resolution. Optical sectioning produced Z-stacks bounded by the extent of fluorescent immunolabeling throughout the thickness of each section. Using Zen software (Carl Zeiss, RRID SCR_013672), PV neurons in each confocal stack were identified and assessed for the presence of a nucleus and whether the entire neuron was within the boundaries of the field of view; only these PV neurons were included in the analysis. The optical slice through the nucleus at which the ellipsoidal minor axis length of each PV neuron reached its maximum was determined. A Z-stack of that optical slice plus one optical slice above and one below was created resulting in a 1.15 µm Z-stack through the middle of each PV neuron; these subset Z-stacks were used for puncta apposition analysis.

Image analysis of GABAergic and glutamatergic appositions onto PV-labeled neurons was performed using Imaris 8.0 software (BitPlane USA, Concord, MA, RRID: SCR_007370) on an offline workstation in the Advanced Light Microscopy Core at Oregon Health & Science University by a blinded observer. For each PV neuron, the manual setting of the *Surfaces* segmentation tool was used to trace the outline of the PV neuron in all three optical slices and a surface was created. To limit our analyses to the area immediately surrounding each PV neuron, we used the *Distance Transform* function followed by the automated *Surfaces* segmentation tool to create another surface 1.5 µm away from the PV neuron surface that followed the unique contours of that PV neuron. The *Mask Channel* function was then used to

only examine WFA, GAD65/67 and VGluT1 within this 1.5 µm-wide perimeter surrounding the PV neuron surface.

The presence of WFA labeling in close proximity to the PV neuron surface was assessed for each PV neuron. A PV neuron was considered to have a PNN if there was any WFA labeling around any part of the PV neuron surface as seen by the observer. GAD65/67 and VGluT1-labeled puncta were then assessed separately using the *Spots* segmentation tool. Within the *Spots* tool, the *Different Spot Sizes (Region Growing)* option was selected and initial settings included an estimated X-Y diameter of 0.5 µm and an estimated Z plane diameter of 0.4 µm. Spots generated by Imaris from these initial settings were then thresholded using the *Classify Spots*, *Quality Filter* histogram to ensure that all labeled puncta were included and background labeling was filtered out. The spots were then thresholded using the *Spot Region, Region Threshold* histogram to ensure that the sizes of the Imaris-generated spots were good approximations of the size of the labeled puncta seen visually by the human observer. Using the *Find Spots Close to Surface Imaris XTension*, we then isolated those spots that were within 0.5 µm of the PV neuron surface. All segmented spots close to the PV neuron surface had to have a Z diameter of at least 0.4 µm to be considered puncta (Hegarty et al., 2010; Hegarty et al., 2014).

*Liquid Chromatography-Mass Spectrometry (LC-MS)*

Freeze-dried brain samples were defatted with 0.5 ml acetone for 30 min vortex and dried in the hood. Each defatted sample was digested in 0.2 ml of Actinase E (2.5 mg/ml) in 55 °C until all the tissue are dissolved (~48 h). After centrifugation at 12,000 rpm, each supernatant was collected and purified by Mini Q spin columns. Protein contaminates were washed out by 0.2 ml of 0.2 M NaCl for 3 times, and the glycosoaminoglycans (GAGs) were eluted from SAX spin column by 0.5 ml of 16% NaCl. Samples eluted from Mini Q spin column were desalted by passing through a 3 kDa molecule weight cut off spin column and washed twice with distilled water. The desalted samples were dissolved in 150 µl of digestion buffer (50 mM ammonium acetate containing 2 mM calcium chloride adjusted to pH 7.0) in filtration units. Recombinant heparin lyases I, II, II (pH optima 7.0-7.5) and recombinant chondroitin lyase ABC (10 mU each, pH optimum 7.4) were added to each sample and mixed well. The samples were all placed in a water bath at 37 °C for 2 h. The enzymatic digestion was terminated by removing the enzymes by centrifugation. The filter unit was washed twice with 100 µl distilled water and the filtrates containing the disaccharide products were lyophilized. The dried samples were AMAC-labeled

by adding 10 µl of 0.1 M AMAC in DMSO/acetic acid (17/3, V/V) incubating at room temperature for 10 min, followed by adding 10 µl of 1 M aqueous $NaBH_3CN$ and incubating for 1 h at 45 °C. A mixture containing all 17-disaccharide standards prepared at 6.25 ng/ul was similarly AMAC-labeled and used for each run as an external standard. After the AMAC-labeling reaction, the samples were centrifuged and each supernatant was recovered. LC was performed on an Agilent 1200 LC system at 45 °C using an Agilent Poroshell 120 ECC18 (2.7 µm, 3.0 x 50 mm) column. Mobile phase A (MPA) was 50 mM ammonium acetate aqueous solution, and the mobile phase B (MPB) was methanol. The mobile phase passed through the column at a flow rate of 300 µl/min. The gradient was 0-10 min, 5-45% B; 10-10.2 min, 45-100% B; 10.2-14 min, 100% B, 14-22 min, 100-5% B. Injection volume is 5 µl. A triple quadrupole MS system equipped with as ESI source (Thermo Fisher Scientific, San Jose, CA) was used a detector. The online mass spectrometric analysis was at the Multiple Reaction Monitoring mode. Mass spectrometry parameters were: negative ionization mode with spray voltage of 3000 V, a vaporizer temperature of 300 °C, and a capillary temperature of 270 °C.

*Whole-cell Patch Clamp Electrophysiology*

For whole-cell patch clamp, rats were anesthetized with isoflurane 2 h after the last saline or cocaine injection followed by intracardial perfusion with a recovery solution oxygenated with 95% $O_2$-5% $CO_2$ at ice-cold temperatures. The composition of the recovery solution was (in mM): 93 NMDG, 2.5 KCl, 1.2 $NaH_2PO_4$, 30 $NaHCO_3$, 20 HEPES, 25 glucose, 4 sodium ascorbate, 2 thiourea, 3 sodium pyruvate, 10 $MgSO_4(H_2O)_7$, 0.5 $CaCl_2(H_2O_2)$, and HCl added until pH was 7.3-7.4 with an osmolarity of 300-310 mOsm. Following perfusion, rats were decapitated, and coronal slices (300 µm) containing the prelimbic PFC (approximately 3.2-3.7 from bregma) were sliced as previously described (Slaker et al., 2015) in ice-cold recovery solution using a vibratome (Leica VT1200S). Prior to recording, slices were incubated for 1 h in room temperature holding solution oxygenated with 95% $O_2$-5% $CO_2$. The composition of holding solution was (in mM): 92 NaCl, 2.5 KCl, 1.2 $NaH_2PO_4$, 30 $NaHCO_3$, 20 HEPES, 25 glucose, 4 sodium ascorbate, 2 thiourea, 3 sodium pyruvate, 2 $MgSO_4(H_2O)_7$, 2 $CaCl_2(H_2O_2)$, and 2 M NaOH added until pH reached 7.3-7.4 and osmolarity was 300-310 mOsm. Immediately before recording, slices were incubated in room temperature holding solution containing WFA (1 µg/ml) for 5 min to stain for PNNs. Each slice was transferred to the recording chamber and fixed to the bottom of the chamber using a platinum harp. The recording chamber was perfused constantly at 31.0 °C at a rate of 4-7 ml/min of aCSF. The aCSF composition was as follows (in mM): 119 NaCl, 2.5 KCl, 1 $NaH_2PO_4$, 26 $NaHCO_3$, 11 dextrose,

1.3 $MgSO_4(H_2O)_7$, and 2.5 $CaCl_2(H_2O)_2$. CellSens software (Olympus) was used to identify fluorescing cells so neurons surrounded by PNNs could be patched. Patching pipettes were pulled from borosilicate capillary tubing (Sutter Instruments, CA USA) and the electrode resistance was typically 4-7 mOhms. Cells were current-clamped at -70 mV and 10 current steps were injected starting at -100pA and ending at 800pA. Elicited action potentials were recorded, counted, and analyzed using pClamp10.3. (Clampfit, Axon Instruments, Sunnyvale, CA).

Mini Analysis (Synaptosoft, Fort Lee, NJ) was used to measure miniature amplitudes and frequencies. To record miniature inhibitory postysynaptic currents (mIPSCs), perfusing aCSF bath contained: 6,7-dinitroquinoxaline-, 2,3-dione (DNQX; 10 μM) and strychnine (1 μM), and tetrodotoxin (1μM) to block AMPA, sodium, and glycine and sodium receptors/channels, respectively. The composition of the intracellular solution was (in mM): 117 CsCl, 2.8 NaCl, 5 $MgCl_2$, 20 HEPES, 2 $Mg^{2+}$ATP, 0.3 $Na^{2+}$GTP, 0.6 EGTA, and sucrose to bring osmolarity to 275-280 mOsm and pH to ~7.25. To record miniature excitatory postsynaptic currents (mEPSCs), aCSF contained picrotoxin (100 μM) and tetrodotoxin (1 μM). Patch pipettes were filled with (in mM): 125 KCL, 2.8 NaCl, 2 $MgCl_2$, 2 ATP-$Na^+$, 0.3 GTP-$Li^+$, 0.6 EGTA, and 10 HEPES. Cells were voltage-clamped at -70 mV and input resistance and series resistance were monitored throughout experiments. IPSCs and EPSCs were amplified and recorded using pClamp10.3. Mini Analysis Program Demo (Synaptosoft Inc, GA USA) was used to measure the peak mIPSC amplitudes or peak mEPSC amplitude.

*Statistical Analysis*

All statistical tests were conducted using Prism6 software (Graph Pad, Inc.). A two-way ANOVA with repeated measure over day was used to assess changes in locomotor activity following cocaine exposure and electrophysiological measures. In the case of a significant interaction, a Sidak's test was used for multiple comparisons. Two-tailed, Student's t-tests were used to compare the number of $WFA^+/PV^+$ cells between treatment conditions (see Table 1). A Kolmogorov-Smirnoff nonparametric test for distribution was used to compare the intensity of WFA and PV among treatment conditions and also for miniature analyses. A Mann-Whitney U test was used for puncta analysis. Correlation between WFA and PV intensity and between cocaine-induced locomotor activity and WFA/PV intensity were done using linear regression analysis. Significance was determined at $p < 0.05$.

## Results

*Cocaine exposure induces locomotor activity*

Figure 1A shows the timeline for all experiments. We show the locomotor activity of every rat used in these studies after acute and repeated saline or cocaine, the latter of which produces behavioral sensitization (Robinson and Berridge, 1993). Figure 1B indicates that locomotor activity increased following acute cocaine injection compared to the habituation day. There was a significant Treatment x Time interaction ($F_{1,63}$ = 8.96, p = 0.0039; N = 31-34/group). Figure 1C shows the locomotor response each day after 5 days of cocaine exposure. There was a trend toward a main effect of Treatment ($F_{1,60}$ = 3.88, p = 0.053; N = 30-32/group) and a significant Treatment x Time interaction ($F_{5,300}$ = 3.52, p = 0.004). Sidak's post-hoc analysis indicated that, compared with the habituation day and the saline controls, cocaine elevated locomotor activity on days 4 and 5. In addition, activity was higher on day 5 cocaine compared with day 1 cocaine, indicating that locomotor sensitization had occurred.

*Cocaine exposure alters intensity of WFA and PV staining within the prelimbic and infralimbic PFC*

WFA is a common marker for PNNs (Hartig et al., 1992) and has been used as an indirect measure of maturity of PNNs (Foscarin et al., 2011; Cabungcal et al., 2013a; Chen et al., 2015; Vazquez-Sanroman et al., 2015a). To test whether PNNs were altered by cocaine exposure, we assessed both intensity and number of PV stained cells with or without WFA surrounding these cells after 1 day or 5 days of saline or cocaine exposure. Linear regression analyses were conducted to determine whether there was a correlation between cocaine-induced locomotor activity and WFA and/or PV staining intensity. All significant correlations are shown in the table in Figure 1-1. The strongest correlations were found in the prelimbic PFC between $WFA^+/PV^+$ cells 2 h after 5 days of cocaine exposure and cocaine-induced locomotor behavior on Day 2 ($p < 0.0001$) and Day 3 ($p = 0.0032$) (Day 2 results are shown in Figure 1D). While there was no

correlation with Day 1 cocaine-induced behavior, ($p = 0.4998$), Days 2 and 3 were strongly correlated, Day 4 was not significant ($p = 0.1793$), and Day 5 was nearly significant ($p = 0.0633$). In the same animals, we also found a correlation between the intensity of single-labeled WFA cells ($WFA^+/PV^-$ cells) with behavior on Day 2 ($p= 0.0138$) and Day 3 ($p = 0.0430$). This finding suggests that an increase in WFA around PV cells may occur early and that the increase may be sustained up to 5 days later, when PNNs were measured. This effect appeared only at 2 h and did not persist in animals assessed 24 h later. Other correlations found in the prelimbic PFC were from rats given 5 days of cocaine exposure and assessed 24 h later. In these rats, there was a weak negative correlation in single-labeled WFA cells with Day 1 cocaine-induced locomotor activity ($p = 0.0462$). In this same group of rats, there was also a negative correlation in the prelimbic PFC between PV staining ($PV^+/WFA^+$ and $PV^+/WFA^-$ cells) with Day 1 cocaine-induced locomotor activity ($p = 0.0124$ and $p = 0.0364$, respectively). None of the correlations we observed in the prelimbic PFC were observed in the infralimbic PFC. In the infralimbic PFC, we found a negative correlation after acute cocaine between staining of WFA in both $WFA^+/PV^+$ and $WFA^+/PV^-$ cells with locomotor activity 24 h later ($p = 0.0146$ and $p = 0.0267$, respectively). There was also a positive correlation between WFA staining in $WFA^+/PV^-$ cells and locomotor activity 2 h after Day 5 of cocaine exposure ($p = 0.0125$). In addition, we found a positive correlation between staining of WFA in both $WFA^+/PV^+$ and $WFA^+/PV^-$ cells and 24 h after Day 3 cocaine-induced activity ($p = 0.0363$ and $p = 0.0170$, respectively. There were no correlations between PV staining and cocaine-induced activity in the infralimbic PFC.

Figure 1E is a photomicrograph of PV single-labeled cells and PV double-labeled cells with WFA to stain for PNNs. We also examined whether there was a correlation between the intensity of PV and WFA staining in the prelimbic and infralimbic PFC. Previous studies have shown that weakly stained PV cells tend to lack PNNs, and digestion of PNNs with Ch-ABC decreases PV levels (Yamada et al., 2014), suggesting that the expression of PNNs impacts the expression of PV or vice-versa. In nearly all cases in both the prelimbic and infralimbic PFC, we found a positive correlation between the intensity of WFA and PV within the same cells; an example of this correlation for the prelimbic PFC 24 h after 5 days of treatment is shown in Figure 1E (saline $R^2 = 0.74$; $p < 0.0001$; cocaine $R^2 = 0.73$, $p < 0.0001$).

Figure 2 shows the distribution of intensity of WFA and PV staining in the prelimbic PFC, with insets showing the same data represented in bar graphs for ease of visibility. Figures 2A and B

show the distribution of intensity of WFA staining around PV cells ($WFA^+/PV^+$ cells, Figure 2A) and WFA single-labeling intensity ($WFA^+/PV^-$ cells, Figure 2B). At 2 h after acute cocaine, we observed a decrease in the intensity of both $WFA^+/PV^+$ cells (Fig. 2A, $p = 0.0002$) and $WFA^+/PV^-$ cells (Figure 2B, $p < 0.0001$). In contrast, after repeated cocaine, the intensity of $WFA^+/PV^-$ cells was increased ($p = 0.0033$) 2 h later. After either acute or repeated cocaine, there were no differences in $WFA^+/PV^+$ or $WFA^+/PV^-$ cell intensity 24 h later (Figure 2A and B, respectively). Thus, 1 day of cocaine exposure rapidly (2 h) decreased WFA intensity, while 5 days of cocaine exposure produced the opposite effect, indicating that PNNs in the prelimbic PFC are differentially altered by acute vs. chronic exposure to cocaine.

PV cells are important regulators of learning and memory, with PV expression levels relatively low during learning and relatively high after memory consolidation (Donato et al., 2013; Favuzzi et al., 2017). Figures 2C and D show the distribution of intensity of PV staining in $PV^+/WFA^+$ cells and $PV^+/WFA^-$ cells in the prelimbic PFC. After 1 day of cocaine, there was a trend toward a decrease in PV intensity in $PV^+/WFA^+$ cells 2 h later (Figure 2C, $p = 0.0792$), and a small but significant decrease in $PV^+/WFA^-$ cells at this time point (Figure 2D, $p = 0.0067$). These decreases were maintained 24 h later, again with a trend toward a decrease in intensity of $PV^+/WFA^+$ cells ($p = 0.0700$), and a significant decrease in intensity of $PV^+/WFA^-$ cells ($p = 0.0164$). After 5 days of cocaine, PV intensity was *increased* 2 h later for both $PV^+/WFA^+$ cells ($p < 0.0001$) and $PV^+/WFA^-$ cells ($p = 0.005$), primarily due to a larger number of cells with less intense staining in the saline group. This increase was maintained 24 h later for $PV^+/WFA^+$ cells ($p = 0.0137$). Thus, similar to the effects of cocaine on WFA intensity, 1 day and 5 days of cocaine exposure produced opposite effects on PV intensity.

Figure 3 shows the distribution of intensity of WFA and PV staining in the infralimbic PFC, with insets showing the same data represented in bar graphs for ease of visibility. Figures 3A and B show the distribution of intensity of WFA staining around PV cells ($WFA^+/PV^+$ cells, Fig. 3A) and WFA single-labeling intensity ($WFA^+/PV^-$ cells, Fig. 3B). At 2 h after acute cocaine, there was a small but significant decrease in $WFA^+/PV^-$ cells (Fig. 3B, $p = 0.0036$). After repeated cocaine, there was an increase in $WFA^+/PV^+$ cells at this same time point. After 24 h, there was a trend toward intensity of $WFA^+/PV^-$ cells ($p = 0.0701$) and a significant increase in $WFA^+/PV^-$ cells after acute cocaine ($p = 0.0124$).

Figures 3C and D show the distribution of PV intensity staining in $PV^+/WFA^+$ and $PV^+/WFA^-$ cells in the infralimbic PFC. Acute cocaine slightly but significantly increased the intensity of $PV^+/WFA^+$ cells (Fig. 2C, $p = 0.0392$) 2 h later, while repeated cocaine increased the intensity of both $PV^+/WFA^+$ cells ($p < 0.0001$) and $PV^+/WFA^-$ cells ($p < 0.0001$) at this same time point. At 24 h, following acute cocaine, the intensity of both $PV^+/WFA^+$ cells ($p = 0.0002$) and $PV^+/WFA^-$ cells ($p = 0.0018$) was decreased, and there were no changes 24 h after repeated cocaine. Thus, changes in the infralimbic were similar to those of the prelimbic in most, but not all, conditions.

We also determined whether cocaine altered the *number* of double-labeled PV cells surrounded by WFA (Table 1). While there were more PV/WFA double-labeled cells in the prelimbic region of the PFC compared with the infralimbic region, there were no differences in these PV/WFA double-labeled cells between saline and cocaine-treated rats within either the prelimbic PFC or the infralimbic PFC.

*Cocaine exposure increases inhibitory and excitatory puncta on PV/WFA cells*

Due to the well-described role of the prelimbic PFC projections to the nucleus accumbens in modulating cocaine-seeking behavior (McFarland and Kalivas, 2001; McLaughlin and See, 2003; McFarland et al., 2004; Ma et al., 2014), and our studies describing a key role for PNNs in the prelimbic but not the infralimbic PFC in cocaine-induced CPP (Slaker et al., 2015), we focused all remaining studies on the prelimbic PFC. To test whether cocaine exposure altered the type of input onto PV cells with PNNs within the prelimbic PFC, we measured GAD65/67-labeled inhibitory and VGluT1-labeled excitatory puncta near PV cells 2 h following 1 day or 5 days of cocaine exposure. Figures 4A - F show a representative example of a PV-labeled cell surrounded by a WFA-labeled PNN (Figure 4A) that is apposed by GAD65/67 (Figure 4C, green arrowheads) and VGluT1 (Figure 4E, magenta arrowheads) puncta as well as how the analysis was conducted in Imaris (Figures 4B, D, F). The number of GAD65/67 puncta apposed to PV cells increased after both 1 day (Figure 4G; $p = 0.0073$) and 5 days (Figure 4K; $p = 0.0018$) of cocaine exposure. The number of VGluT1 puncta did not change after 1 day of cocaine (Figure 4H) or after 5 days of cocaine exposure (Figure 4L). There was a trend toward an increased ratio of GAD65/67:VGluT1 puncta near PV cells surrounded by WFA after 1 day cocaine exposure (Fig. 4I; $p = 0.0911$), and this ratio was significantly increased after 5 days of cocaine exposure (Figure 4M; $p = 0.0407$), suggesting that there was an increase in the inhibitory:excitatory ratio after repeated cocaine exposure. Inasmuch as these puncta represent

new or impending synapse formation, our findings suggest that new inputs onto PV cells may occur rapidly (within 2 h). We also found an approximate 10% decrease in PV cell volume after 1 day of cocaine exposure (Figure 4J; $p = 0.0288$) with no changes after 5 days of cocaine exposure.

*Electrophysiology*

We used whole-cell electrophysiology to determine whether an acute (1 day) or repeated (5 day) cocaine exposure influenced intrinsic excitability and/or synaptic transmission onto PNN-surrounded neurons in the deeper layers (V and VI) of the prelimbic PFC (Figure 5A). The FSIs in this region of the cortex are highly likely to be PV-containing cells (Kawaguchi and Kubota, 1993). We recently found that > 90% of FSIs recorded in these layers were surrounded by PNNs (unpublished results). All recordings were made 2 h following acute (1 day) or repeated (5 day) cocaine exposure. Figure 5B shows that the number of current-induced action potentials was decreased after acute and repeated cocaine compared with saline controls for WFA-labeled FSIs in the prelimbic PFC. There was a Treatment effect ($F_{2,61} = 7.72$, $p < 0.001$), a Time effect ($F_{8,488} = 1150$, $p < 0.001$), and a Treatment x Time Interaction ($F_{16,488} = 6.72$, $p < 0.001$). Sidak's post-hoc analysis indicated that both acute and repeated cocaine attenuated the number of action potentials elicited relative to saline controls. The decrease after acute cocaine was observed after low levels of injected current, while the decrease after repeated cocaine was observed at higher levels of injected current (> 500 pA). Figure 5D shows a trace example of the first elicited action potential from rats treated with either saline or acute or repeated cocaine. Following acute cocaine, the action potential amplitude was decreased (Figure 5I; $p = 0.0170$), and following repeated cocaine, the resting membrane potential was decreased (Figure 5E; $p = 0.0295$), the half-width of action potentials was increased (Figure 5J; $p = 0.0170$), and the rise time was increased (Figure 5H; $p = 0.0272$). There were no differences between saline and cocaine groups for input resistance (Figure 5F), action potential threshold (Figure 5G), or action potential after hyperpolarization (Figure 5K).

Additionally, we used miniature recordings to determine whether cocaine exposure influenced synaptic transmission onto PNN-surrounded FSIs. Pharmacological tools allowed us to isolate glutamatergic and GABAergic transmission. Figure 5L shows the mEPSC amplitude and frequency after cocaine treatment. We found that acute cocaine produced a small but significant increase in mEPSC amplitude ($p < 0.0001$), but that repeated cocaine decreased the mEPSC

amplitude ($p < 0.0001$). The frequency of the mEPSC inter-event interval was decreased after both acute ($p < 0.0001$) and repeated ($p < 0.0001$) cocaine, suggesting greater excitatory input onto PV cells surrounded by WFA. Figure 5M shows the mIPSC amplitude and frequency after cocaine treatment. Acute cocaine treatment decreased the mIPSC amplitude ($p < 0.0001$) but, in contrast, repeated cocaine increased the mIPSC amplitude ($p < 0.0001$). The frequency of the mIPSC inter-event interval was increased after acute cocaine ($p < 0.0001$) but was decreased after repeated cocaine ($p = 0.0015$). Overall, these findings indicate that, while repeated cocaine may increase both excitatory and inhibitory input onto FSIs, the postsynaptic excitatory response is reduced, and the combination of both an increase in inhibitory input and an increase in mIPSC amplitude would be expected to inhibit the output of FSIs.

*Composition of glycosaminoglycans, hyaluronic acid, and chondroitin sulfates following a single or repeated cocaine exposure*

PNNs are composed of interacting glycosaminoglycans (GAGs). Hyaluronic acid (HA) is produced in the membrane and extruded to produce an ECM backbone to which chondroitin and heparin sulfate proteoglycans (CSPG and HSPG, respectively) are bound and stabilized through link proteins. The position of the sulfate groups on CSPGs changes patterns during development (Carulli et al., 2010), with the 0S and 6S positions prevalent during periods of high plasticity and the 4S position being dominant during periods of low plasticity (Carulli et al., 2010). Here we determined the impact of 1 day or 5 days of saline or cocaine treatment on GAGs, HA, and CSs 2 h later. We used mPFC brain punches, which comprised primarily the prelimbic PFC but also some portions of the infralimbic PFC. Table 2 shows that approximately half of the total GAG composition was in the form of chondroitin sulfate (CS), with the remaining half being both heparin sulfate (HS) and HA. This population did not shift 2 h after acute or repeated cocaine exposure. We also assessed the sulfation patterns of CSs and HSs. For CSs, the 4S position was the most prevalent sulfation position (90%). However, there was no difference between treatment groups for sulfate position on CSs. Additionally, on HSs, the 0S position was the most prevalent sulfation position, with over 60% of all sulfates at this position. There was no difference between treatment groups for sulfate position on HSs (Table 2). Thus, the changes in PNNs found after cocaine exposure were not reflected in measurements that included both PNNs and the loose ECM.

## Discussion

Recent studies have shown that other drugs of abuse (cocaine, heroin, nicotine, and alcohol) alter the intensity of PNNs and/or their components, with the direction of the changes dependent on the drug, the extent of exposure and withdrawal, and the brain region (Van den Oever et al., 2010b; Coleman et al., 2014; Vazquez-Sanroman et al., 2015b; Carbo-Gas et al., 2017; Vazquez-Sanroman et al., 2017). However, the *functional* state of PV FSIs surrounded by PNNs has not been investigated. Here we provide evidence that PNN and PV labeling intensity respond to cocaine exposure with temporal specificity in the prelimbic PFC and infralimbic PFC. Changes in the intensity of PNNs and PV occurred within 2 h of a single cocaine exposure and generally paralleled each other, with PV intensity changes occurring several hours after PNN changes. Acute cocaine decreased PNN and PV intensity, while repeated cocaine increased PNN and PV intensity. In the prelimbic PFC, acute cocaine decreased the excitability of FSIs surrounded by PNNs, but inconsistent with this decreased excitability, produced synaptic changes indicative of increased glutamate release and decreased GABA release from inputs to these cells. This disconnect between quantal input to the cell and the overall excitability could be due to changes in the efficacy of ionic influx after quantal events, perhaps due to changes in intracellular levels of PV, which functions as a calcium buffer (Caillard et al., 2000). However, repeated cocaine exposure produced changes consistent with decreases in PV/PNN cell excitability after cocaine, including a decrease in evoked action potentials of FSIs, an increase in the ratio of GAD65/67:VGluT1 puncta, an increase in both the frequency and amplitude of mIPSCs, and a reduction in mEPSC amplitudes.

*Cocaine-induced changes in PNN and PV intensity*

Previous work reported a positive correlation between the intensity of PV and PNNs (Yamada et al., 2014), in accordance with our current findings. Cocaine-induced changes in PV intensity generally followed those in PNNs, suggesting a potential codependence of PV and PNNs. PNNs are believed to protect underlying PV neurons from oxidative stress (Cabungcal et al., 2013b), and a higher firing frequency in PV FSIs may require higher PV content to bind intracellular calcium and promote activity-dependent production of PNNs (Dityatev et al., 2007) that sequester calcium (Bruckner et al., 1993). Recent work demonstrated that experience alters the activity of PV cells in the hippocampus through the PNN component brevican (Favuzzi et al., 2017), which mediates changes through altered AMPA receptors and voltage-gated potassium channels critical for fast-spiking of PV cells. While we did not measure individual CSPGs within

PNNs, we assessed total GAG composition in the total ECM (which includes PNNs) from tissue punches containing the prelimbic PFC. No changes in these components were found after acute or repeated cocaine, suggesting that any changes in PNN intensity are likely specific to these structures rather than to the loose ECM.

In some instances, we found a correlation between the intensity of WFA or PV staining and cocaine-induced locomotor behavior in the prelimbic and infralimbic PFC (Figure 1-1). The strongest correlations and most consistently observed changes appeared to be in $WFA^+/PV^+$ cells in the prelimbic PFC just 2 h after 5 days of cocaine exposure. WFA staining around PV cells was strongly correlated with Days 2 and 3, and nearly correlated with Day 5 of cocaine-induced locomotor activity, suggesting that locomotor activity after cocaine injection on Days 2 and 3 may reflect cocaine-induced plasticity within PNNs that in turn shape prelimbic PFC output to modulate locomotor activity.

*Cocaine-induced changes in intrinsic and synaptic properties of FSIs*

The findings here expand on our previous study in which we found that repeated cocaine reduced the mIPSC frequency onto pyramidal neurons in the prelimbic PFC (Slaker et al., 2015). This attenuation may be due to a cocaine-induced reduction in firing of PNN-surrounded PV neurons mediated by increased GABA release and increased postsynaptic responsiveness to GABA on these PV neurons, along with an increase in the ratio of GAD65/67:VGluT1 puncta. Of note, our analysis accounted for puncta only around the cell body that may not reflect changes in dendrites contributing to firing.

The electrophysiological findings in FSIs, which are likely PV-containing cells (Kawaguchi and Kubota, 1993), are consistent with the idea that an increase in the inhibitory:excitatory balance onto PV/PNN cells reduces inhibitory output to pyramidal neurons, contributing to the hyperexcitability of these neurons that we and others have reported following repeated, noncontingent cocaine (Dong et al., 2005; Nasif et al., 2005; Huang et al., 2007; Hearing et al., 2013; Slaker et al., 2015). These studies are also consistent with the finding that targeted optogenetic stimulation of PV FSIs globally inhibits prelimbic PFC network activity (Sparta et al., 2014). However, previous work showed that a cocaine challenge elevates extracellular GABA levels in the mPFC (Jayaram and Steketee, 2005) in cocaine-sensitized rats, although the contribution by FSIs to the elevated extracellular GABA levels could not be discerned in that

study. FSIs in particular may be modulated by cocaine to quickly shut off activity of pyramidal neurons (Lapish et al., 2007), and repeated cocaine treatment may reduce this ability to inhibit pyramidal neurons.

The changes in electrophysiological properties of FSIs 2 h after repeated cocaine exposure suggest that cocaine alters FSIs differently from paradigms that examine changes after withdrawal from cocaine. Campanac (Campanac and Hoffman, 2013) found that 5 days of cocaine injections followed by 10-13 days of withdrawal increased spike number and attenuated mEPSC amplitude and frequency. We observed a decrease in spike number with a decrease in mEPSC amplitude and an increase in the mEPSC frequency after 5 days of cocaine exposure. Although these studies did not use WFA to label PNNs, a vast majority of these cells likely would have stained positive for WFA because >90% of WFA-labeled neurons are FSIs within layer V of the prelimbic PFC (unpublished results). Together, these findings suggest that both cocaine exposure and subsequent withdrawal influence the intrinsic firing and synaptic transmission of FSIs, but that withdrawal periods facilitate additional plasticity. Nonetheless, the events occurring prior to withdrawal may give clues to the sequence of early events involved in disrupted PV cell-associated circuits contributing to aberrant learning processes after cocaine exposure.

*Mechanistic considerations*

Previous studies have shown that PNNs or their components influence intrinsic firing and synaptic transmission (Dityatev et al., 2007; Van den Oever et al., 2010a; Slaker et al., 2015; Balmer, 2016; Carstens et al., 2016; Favuzzi et al., 2017). Full degradation of PNNs has been shown to both decrease (Balmer, 2016) and increase (Dityatev et al., 2007) the firing of cultured neurons and to impair induction of long-term potentiation (Carstens et al., 2016), with the difference likely dependent on the brain region and time interval after PNN degradation. Our data show that cocaine exposure in the intact brain (no exogenous enzymatic PNN degradation) attenuates firing of PNN-surrounded FSIs in the prelimbic PFC. Thus, cocaine-induced changes in the intensity of PNNs may influence firing, consistent with the above studies in which PNNs are completely degraded and with a recent report demonstrating a role for the PNN component brevican in regulating firing in PV cells and excitatory input onto PV cells, in turn altering intrinsic properties of PV neurons, possibly via Kv1.1 or Kv3.1b channels (Favuzzi et al., 2017). Not readily explainable are our observations that repeated cocaine decreased firing of and

680 increased inhibitory input onto FSIs in the prelimbic PFC at the same time point that we found
681 increased PV and PNN intensity. These findings suggest that transient changes in PNN or PV
682 intensity may not be coordinated temporally with the changes in electrophysiological measures
683 or that the increases in intensity are compensatory responses to cocaine exposure.
684
685 A key mechanism that may link cocaine exposure to changes in PNN and/or PV intensity is
686 cocaine-induced oxidative stress (Dietrich et al., 2005; Jang et al., 2014). A central role for
687 PNNs is their protection of underlying neurons from oxidative stress (Morawski et al., 2004;
688 Cabungcal et al., 2013b; Suttkus et al., 2014). PNNs however, are themselves susceptible to
689 oxidative stress (Cabungcal et al., 2013b). Thus, while the impact of cocaine on PNNs is
690 transient and may occur in response to oxidative stress, these responses may set the stage for
691 a cascade of downstream consequences, including partial degradation of PNNs that allows for
692 new synaptic inputs onto PV cells after acute cocaine. The acute cocaine-induced decrease in
693 PV cell volume in the prelimbic PFC may reflect a cocaine-induced oxidative stress effect. In
694 contrast, the increase in PNN intensity after repeated cocaine, although relatively small, may
695 restrict new synaptic inputs by binding of inhibitory molecules such as Sema3A, by physical
696 constraints (Wang and Fawcett, 2012; Vo et al., 2013), and/or by restricting the lateral
697 movement of AMPA receptors important for short-term plasticity (Frischknecht et al., 2009). ,
698 Changes in PV cell volume do not appear to underlie changes in PNN intensity or in the intrinsic
699 or synaptic properties after repeated cocaine, since PV cell volumes were not different between
700 saline controls and cocaine-treated rats after repeated cocaine.
701
702 *Conclusions*
703
704 Here we demonstrated that the intensity of PNNs and PV rapidly decrease in the prelimbic and
705 infralimbic PFC following a novel cocaine exposure but increase following repeated cocaine
706 exposure. The decreased PNN intensity in response to a single cocaine injection may promote
707 early changes that enable new synaptic input, recapitulating early development and in
708 accordance with the rejuvenation hypothesis of cocaine addiction (Dong and Nestler, 2014). In
709 the prelimbic PFC, repeated cocaine increases inhibitory input onto PV cells surrounded by
710 PNNs, which in turn may promote the hyperexcitability of pyramidal neurons we and others
711 previously reported and that promote reinstatement to drug-seeking behavior. While some of
712 these changes may be transient, the rapid responses to cocaine may alter network stability of
713 PV FSIs that partially set into motion the persistent and chronic nature of drug addiction.

714 Importantly, PV FSIs drive gamma oscillations that promote cognitive processing (Womelsdorf et al.,
715 2007; Sohal et al., 2009) and adaptations in these PV FSIs may also underlie the cognitive impairment
716 in cocaine addicts (Potvin et al., 2014).
717
718

719 **Figure Legends**
720
721 **Figure 1. Cocaine exposure increases locomotor activity and PV intensity is correlated with**
722 **WFA intensity**. Data are mean ± SEM. **(A)** Timeline of experiment. **(B)** Infrared photocell beam
723 breaks the first 15 min after saline or cocaine (15 mg/kg, ip) injection. A single cocaine exposure
724 increased the locomotor response compared with the habituation (Hab) day. **(C)** Repeated cocaine
725 increased locomotor activity compared with their Hab day and with saline controls on D4 and D5.
726 **(D)** Significant positive correlation between WFA staining intensity in $WFA^+/PV^+$ cells and cocaine-
727 induced locomotor activity on Day 2 when intensity was examined 2 h after 5 days of cocaine
728 exposure (see Figure 1-1 for all correlations). **(E)** Representative photomicrograph of PV cells (Red)
729 with (yellow arose) and without (blue arrows) WFA (green). WFA was also observed surrounding
730 non-PV cells (white arrows). Scale bar = 100 µm. **(F)** Significant positive correlation between WFA
731 and PV intensity in rats 24 h after 5 days of saline (open circles) or cocaine (closed circles). For B
732 and C: * $p < 0.05$, compared to saline group; +$p < 0.05$, compared to Hab group.
733
734 **Figure 2. Cocaine exposure alters intensity of WFA and PV in the *prelimbic PFC*.**
735 **(A)** Intensity of WFA surrounding PV cells ($WFA^+/PV^+$ cells) and **(B)** intensity of WFA surrounding all
736 non-PV cells ($WFA^+/PV^-$ cells) 2 h or 24 h after acute (1 day) or repeated (5 day) saline (S) or
737 cocaine (C) in the prelimbic PFC. **(C)** Intensity of PV cells that are surrounded by WFA ($PV^+/WFA^+$
738 cells) and **(D)** intensity of $PV^+/WFA^-$ cells 2 or 24 h after acute or repeated saline or cocaine. N = 6-
739 8 rats/group. * $p < 0.05$, compared to saline group.
740
741 **Figure 3. Cocaine exposure alters intensity of WFA and PV in the *infralimbic PFC*.**
742 **(A)** Intensity of WFA surrounding PV cells ($WFA^+/PV^+$ cells) and **(B)** intensity of WFA surrounding all
743 non-PV cells ($WFA^+/PV^-$ cells) 2 h or 24 h after acute (1 day) or repeated (5 day) saline (S) or
744 cocaine (C) in the infralimbic PFC. **(C)** Intensity of PV cells that are surrounded by WFA ($PV^+/WFA^+$
745 cells) and **(D)** intensity of $PV^+/WFA^-$ cells PV cell intensity at 2 or 24 h after acute or repeated saline
746 or cocaine. N = 6-8 rats/group. * $p < 0.05$, compared to saline group.
747
748 **Figure 4. Cocaine alters intensity of GABAergic (GAD65/67) puncta near PV neurons**
749 **surrounded by PNNs in the prelimbic PFC.** Cells were visualized with confocal microscopy
750 and analyzed using Imaris segmentation tools. **(A)** Representative PV neuron (red) surrounded
751 by a PNN labeled with WFA (blue). **(B)** The PV neuron is traced and a Surface is created. **(C)**
752 The Mask Channel function was used to isolate GAD65/67 labeling to the area outside of the

PV neuronal surface and GAD65/67-labeled puncta (green arrowheads) were identified. **(D)** GAD65/67-labeled puncta (green arrowheads) were then thresholded using the Imaris Spots tool. Spots that met size criteria and were located adjacent to the PV neuron Surface were included in the analysis (green arrows). **(E)** VGluT1-labeled puncta (magenta arrowheads) were segmented separately using the same protocol and **(F)** VGluT1 Spots meeting our size and location criteria were included in the analysis (magenta arrows). **(G)** 1 day of cocaine increases GAD 65/67 puncta (saline N = 3, 45 cells; cocaine N = 3, 49 cells), **(H)** no change in VGluT1 puncta, and **(I)** a trend toward an increase in the ratio of GAD65/67:VGluT1 puncta. **(J)** 1 day of cocaine decreases PV cell volume. **(K)** 5 days of cocaine increases GAD 65/67 puncta (saline N = 4, 49 cells; cocaine N = 6, 78 cells), **(L)** no change in VGluT1 puncta, **(M)** 5 days of cocaine increases the ratio of GAD65/67:VGluT1 puncta. **(N)** 5 days of cocaine does not alter PV cell volume. Data from bar graphs are mean ± SEM. Scale bar = 3 μm. *p < 0.05 and #p < 0.1, compared with saline controls.

**Figure 5. Intrinsic and synaptic properties of FSIs surrounded by PNNs exposed to cocaine in the prelimbic PFC.** Data are mean ± SEM. Fast-spiking interneuron properties 2 h following 1 day or 5 days of saline or cocaine. **(A)** Recording locations in layer V of the prelimbic PFC. **(B)** Action potentials recorded from FSIs surrounded by WFA. *p < 0.0001 comparing between saline and both cocaine groups; +p < 0.0001 comparing between saline and 1 day cocaine. **(C)** Trace examples of recorded FSIs at 800 pA. Scale bar represents 50 ms, 50 mV. **(D)** Trace example of first elicited action potential (AP). Dashed = saline, gray = 1 day cocaine, black = 5 days cocaine. Scale bar represents 20 mV, 500 μs. **(E-K)** Intrinsic properties: (E) Resting membrane potential, (F) Input resistance, (G) AP threshold, (H) rise time, (I) AP amplitude, (J) AP half-width, and (K) AP afterhyperpolarization potential, comparing acute and repeated cocaine (C) to acute and repeated saline controls (S), respectively. **(L)** Cumulative frequency plots of mEPSC amplitudes and inter-event intervals. Trace examples are shown below. Scale bar represents 50 pA, 500 μs. **(M)** Cumulative frequency plots of mIPSC amplitudes and inter-event intervals. Trace examples are shown below. The number of cells/number of rats used is shown (E, L, M).

**Figure 1-1. Table showing significant correlations between cocaine-induced locomotor activity and WFA or PV intensity in single- and double-labeled cells in the prelimbic and infralimbic PFC.**

*Author Contributions*

BAS designed and interpreted the behavioral data and immunohistochemical data for PV and PNN intensity analysis, wrote and revised the manuscript; MLK performed the behavioral components and immunohistochemical analysis for the PV and PNN intensity analysis and wrote the manuscript; DMH performed the immunohistochemistry and Imaris analysis of puncta data and revised the manuscript; SAA designed, analyzed and interpreted the puncta study and revised the manuscript; XL and YK performed the LC-MS analysis, FZ and RJL designed the GAG analysis experiments and helped in writing the manuscript; TEB helped to design and interpret the electrophysiological data and wrote and revised portions of the manuscript, and ETJ performed the electrophysiological experiments and wrote portions of the manuscript.

*Acknowledgements*

This work was supported by National Institutes of Health grants DA033404 and DA040965 (BAS); DA040965 and P30GM103398 (TEB); P30 NS061800 (SAA); NIH DK111958 and HL125371(RJL).

## References


Balmer TS (2016) Perineuronal Nets Enhance the Excitability of Fast-Spiking Neurons. eNeuro 3.

Balmer TS, Carels VM, Frisch JL, Nick TA (2009) Modulation of perineuronal nets and parvalbumin with developmental song learning. The Journal of neuroscience 29:12878-12885.

Banerjee SB, Gutzeit VA, Baman J, Aoued HS, Doshi NK, Liu RC, Ressler KJ (2017) Perineuronal Nets in the Adult Sensory Cortex Are Necessary for Fear Learning. Neuron 95:169-179 e163.

Bruckner G, Brauer K, Hartig W, Wolff JR, Rickmann MJ, Derouiche A, Delpech B, Girard N, Oertel WH, Reichenbach A (1993) Perineuronal nets provide a polyanionic, glia-associated form of microenvironment around certain neurons in many parts of the rat brain. Glia 8:183-200.

Cabungcal JH, Steullet P, Kraftsik R, Cuenod M, Do KQ (2013a) Early-life insults impair parvalbumin interneurons via oxidative stress: reversal by N-acetylcysteine. Biol Psychiatry 73:574-582.

Cabungcal JH, Steullet P, Morishita H, Kraftsik R, Cuenod M, Hensch TK, Do KQ (2013b) Perineuronal nets protect fast-spiking interneurons against oxidative stress. Proceedings of the National Academy of Sciences of the United States of America 110:9130-9135.

Caillard O, Moreno H, Schwaller B, Llano I, Celio MR, Marty A (2000) Role of the calcium-binding protein parvalbumin in short-term synaptic plasticity. Proc Natl Acad Sci U S A 97:13372-13377.

Campanac E, Hoffman DA (2013) Repeated cocaine exposure increases fast-spiking interneuron excitability in the rat medial prefrontal cortex. Journal of neurophysiology 109:2781-2792.

Carbo-Gas M, Moreno-Rius J, Guarque-Chabrera J, Vazquez-Sanroman D, Gil-Miravet I, Carulli D, Hoebeek F, De Zeeuw C, Sanchis-Segura C, Miquel M (2017) Cerebellar perineuronal nets in cocaine-induced pavlovian memory: Site matters. Neuropharmacology 125:166-180.

Carstens KE, Phillips ML, Pozzo-Miller L, Weinberg RJ, Dudek SM (2016) Perineuronal Nets Suppress Plasticity of Excitatory Synapses on CA2 Pyramidal Neurons. The Journal of neuroscience : the official journal of the Society for Neuroscience 36:6312-6320.

Carulli D, Pizzorusso T, Kwok JC, Putignano E, Poli A, Forostyak S, Andrews MR, Deepa SS, Glant TT, Fawcett JW (2010) Animals lacking link protein have attenuated perineuronal nets and persistent plasticity. Brain : a journal of neurology 133:2331-2347.

Chen H, He D, Lasek AW (2015) Repeated Binge Drinking Increases Perineuronal Nets in the Insular Cortex. Alcoholism, clinical and experimental research 39:1930-1938.

848 Coleman LG, Jr., Liu W, Oguz I, Styner M, Crews FT (2014) Adolescent binge ethanol treatment
849 alters adult brain regional volumes, cortical extracellular matrix protein and behavioral
850 flexibility. Pharmacology, biochemistry, and behavior 116:142-151.

851 Dietrich JB, Mangeol A, Revel MO, Burgun C, Aunis D, Zwiller J (2005) Acute or repeated
852 cocaine administration generates reactive oxygen species and induces antioxidant
853 enzyme activity in dopaminergic rat brain structures. Neuropharmacology 48:965-974.

854 Dityatev A, Bruckner G, Dityateva G, Grosche J, Kleene R, Schachner M (2007) Activity-
855 dependent formation and functions of chondroitin sulfate-rich extracellular matrix of
856 perineuronal nets. Developmental neurobiology 67:570-588.

857 Donato F, Rompani SB, Caroni P (2013) Parvalbumin-expressing basket-cell network plasticity
858 induced by experience regulates adult learning. Nature 504:272-276.

859 Dong Y, Nestler EJ (2014) The neural rejuvenation hypothesis of cocaine addiction. Trends
860 Pharmacol Sci 35:374-383.

861 Dong Y, Nasif FJ, Tsui JJ, Ju WY, Cooper DC, Hu XT, Malenka RC, White FJ (2005) Cocaine-
862 induced plasticity of intrinsic membrane properties in prefrontal cortex pyramidal
863 neurons: adaptations in potassium currents. J Neurosci 25:936-940.

864 Favuzzi E, Marques-Smith A, Deogracias R, Winterflood CM, Sanchez-Aguilera A, Mantoan L,
865 Maeso P, Fernandes C, Ewers H, Rico B (2017) Activity-Dependent Gating of
866 Parvalbumin Interneuron Function by the Perineuronal Net Protein Brevican. Neuron
867 95:639-655 e610.

868 Fawcett J (2009) Molecular control of brain plasticity and repair. Progress in brain research
869 175:501-509.

870 Foscarin S, Raha-Chowdhury R, Fawcett JW, Kwok JCF (2017) Brain ageing changes
871 proteoglycan sulfation, rendering perineuronal nets more inhibitory. Aging (Albany NY)
872 9:1607-1622.

873 Foscarin S, Ponchione D, Pajaj E, Leto K, Gawlak M, Wilczynski GM, Rossi F, Carulli D (2011)
874 Experience-dependent plasticity and modulation of growth regulatory molecules at
875 central synapses. PloS one 6:e16666.

876 Frischknecht R, Heine M, Perrais D, Seidenbecher CI, Choquet D, Gundelfinger ED (2009)
877 Brain extracellular matrix affects AMPA receptor lateral mobility and short-term
878 synaptic plasticity. Nature neuroscience 12:897-904.

879 Gogolla N, Caroni P, Luthi A, Herry C (2009) Perineuronal nets protect fear memories from
880 erasure. Science 325:1258-1261.

881 Hartig W, Brauer K, Bruckner G (1992) Wisteria floribunda agglutinin-labelled nets surround
882 parvalbumin-containing neurons. Neuroreport 3:869-872.

883 Hearing M, Kotecki L, Marron Fernandez de Velasco E, Fajardo-Serrano A, Chung HJ, Lujan R,
884 Wickman K (2013) Repeated cocaine weakens GABA(B)-Girk signaling in layer 5/6
885 pyramidal neurons in the prelimbic cortex. Neuron 80:159-170.

886 Hegarty DM, Hermes SM, Largent-Milnes TM, Aicher SA (2014) Capsaicin-responsive corneal
887 afferents do not contain TRPV1 at their central terminals in trigeminal nucleus caudalis
888 in rats. J Chem Neuroanat 61-62:1-12.

889 Hegarty DM, Tonsfeldt K, Hermes SM, Helfand H, Aicher SA (2010) Differential localization of
890 vesicular glutamate transporters and peptides in corneal afferents to trigeminal nucleus
891 caudalis. The Journal of comparative neurology 518:3557-3569.

892 Huang CC, Lin HJ, Hsu KS (2007) Repeated cocaine administration promotes long-term
893 potentiation induction in rat medial prefrontal cortex. Cerebral cortex 17:1877-1888.

894 Jang EY, Ryu YH, Lee BH, Chang SC, Yeo MJ, Kim SH, Folsom RJ, Schilaty ND, Kim KJ, Yang
895 CH, Steffensen SC, Kim HY (2014) Involvement of reactive oxygen species in cocaine-
896 taking behaviors in rats. Addict Biol.

897 Jayaram P, Steketee JD (2005) Effects of cocaine-induced behavioural sensitization on GABA
898 transmission within rat medial prefrontal cortex. The European journal of neuroscience
899 21:2035-2039.

900 Kawaguchi Y, Kubota Y (1993) Correlation of physiological subgroupings of nonpyramidal cells
901 with parvalbumin- and calbindinD28k-immunoreactive neurons in layer V of rat frontal
902 cortex. J Neurophysiol 70:387-396.

903 Kroener S, Lavin A (2010) Altered dopamine modulation of inhibition in the prefrontal cortex of
904 cocaine-sensitized rats. Neuropsychopharmacology : official publication of the
905 American College of Neuropsychopharmacology 35:2292-2304.

906 Kwok JC, Dick G, Wang D, Fawcett JW (2011) Extracellular matrix and perineuronal nets in
907 CNS repair. Developmental neurobiology 71:1073-1089.

908 Lapish CC, Kroener S, Durstewitz D, Lavin A, Seamans JK (2007) The ability of the
909 mesocortical dopamine system to operate in distinct temporal modes.
910 Psychopharmacology 191:609-625.

911 Lee AT, Gee SM, Vogt D, Patel T, Rubenstein JL, Sohal VS (2014) Pyramidal neurons in
912 prefrontal cortex receive subtype-specific forms of excitation and inhibition. Neuron
913 81:61-68.

914 LeMoine C, Gaspar P (1998) Subpopulations of cortical GABAergic interneurons differ by their
915 expression of D1 and D2 dopamine receptor subtypes. Mol Brain Res 58:231-236.

916 Ma YY, Lee BR, Wang X, Guo C, Liu L, Cui R, Lan Y, Balcita-Pedicino JJ, Wolf ME, Sesack SR,
917 Shaham Y, Schluter OM, Huang YH, Dong Y (2014) Bidirectional modulation of
918 incubation of cocaine craving by silent synapse-based remodeling of prefrontal cortex
919 to accumbens projections. Neuron 83:1453-1467.

920 Madinier A, Quattromani MJ, Sjolund C, Ruscher K, Wieloch T (2014) Enriched housing
921 enhances recovery of limb placement ability and reduces aggrecan-containing
922 perineuronal nets in the rat somatosensory cortex after experimental stroke. PloS one
923 9:e93121.

McFarland K, Kalivas PW (2001) The circuitry mediating cocaine-induced reinstatement of drug-seeking behavior. J Neurosci 21:8655-8663.

McFarland K, Davidge SB, Lapish CC, Kalivas PW (2004) Limbic and motor circuitry underlying footshock-induced reinstatement of cocaine-seeking behavior. The Journal of neuroscience : the official journal of the Society for Neuroscience 24:1551-1560.

McLaughlin J, See RE (2003) Selective inactivation of the dorsomedial prefrontal cortex and the basolateral amygdala attenuates conditioned-cued reinstatement of extinguished cocaine-seeking behavior in rats. Psychopharmacology 168:57-65.

Morawski M, Bruckner MK, Riederer P, Bruckner G, Arendt T (2004) Perineuronal nets potentially protect against oxidative stress. Experimental neurology 188:309-315.

Nasif FJ, Sidiropoulou K, Hu XT, White FJ (2005) Repeated cocaine administration increases membrane excitability of pyramidal neurons in the rat medial prefrontal cortex. J Pharmacol Exp Ther 312:1305-1313.

Paxinos G WC (1998) The Rat Brain in Stereotaxic Coordinates, 4 Edition. New York: Academic Press.

Pizzorusso T, Medini P, Berardi N, Chierzi S, Fawcett JW, Maffei L (2002) Reactivation of ocular dominance plasticity in the adult visual cortex. Science 298:1248-1251.

Potvin S, Stavro K, Rizkallah E, Pelletier J (2014) Cocaine and cognition: a systematic quantitative review. J Addict Med 8:368-376.

Robinson TE, Berridge KC (1993) The neural basis of drug craving: an incentive-sensitization theory of addiction. Brain Res Brain Res Rev 18:247-291.

Romberg C, Yang S, Melani R, Andrews MR, Horner AE, Spillantini MG, Bussey TJ, Fawcett JW, Pizzorusso T, Saksida LM (2013) Depletion of perineuronal nets enhances recognition memory and long-term depression in the perirhinal cortex. The Journal of neuroscience : the official journal of the Society for Neuroscience 33:7057-7065.

Slaker M, Churchill L, Todd RP, Blacktop JM, Zuloaga DG, Raber J, Darling RA, Brown TE, Sorg BA (2015) Removal of perineuronal nets in the medial prefrontal cortex impairs the acquisition and reconsolidation of a cocaine-induced conditioned place preference memory. J Neurosci 35:4190-4202.

Slaker ML, Harkness JH, Sorg BA (2016) A standardized and automated method of perineuronal net analysis using Wisteria floribunda agglutinin staining intensity. IBRO Rep 1:54-60.

Sleipness EP, Sorg BA, Jansen HT (2005) Time of day alters long-term sensitization to cocaine in rats. Brain research 1065:132-137.

Sohal VS, Zhang F, Yizhar O, Deisseroth K (2009) Parvalbumin neurons and gamma rhythms enhance cortical circuit performance. Nature 459:698-702.

960 Sparta DR, Hovelso N, Mason AO, Kantak PA, Ung RL, Decot HK, Stuber GD (2014) Activation
961 of prefrontal cortical parvalbumin interneurons facilitates extinction of reward-seeking
962 behavior. The Journal of neuroscience : the official journal of the Society for
963 Neuroscience 34:3699-3705.

964 Suttkus A, Rohn S, Weigel S, Glockner P, Arendt T, Morawski M (2014) Aggrecan, link protein
965 and tenascin-R are essential components of the perineuronal net to protect neurons
966 against iron-induced oxidative stress. Cell death & disease 5:e1119.

967 Van den Oever MC, Spijker S, Smit AB, De Vries TJ (2010a) Prefrontal cortex plasticity
968 mechanisms in drug seeking and relapse. Neurosci Biobehav Rev 35:276-284.

969 Van den Oever MC, Lubbers BR, Goriounova NA, Li KW, Van der Schors RC, Loos M, Riga D,
970 Wiskerke J, Binnekade R, Stegeman M, Schoffelmeer AN, Mansvelder HD, Smit AB,
971 De Vries TJ, Spijker S (2010b) Extracellular matrix plasticity and GABAergic inhibition
972 of prefrontal cortex pyramidal cells facilitates relapse to heroin seeking.
973 Neuropsychopharmacology : official publication of the American College of
974 Neuropsychopharmacology 35:2120-2133.

975 Vazquez-Sanroman D, Leto K, Cerezo-Garcia M, Carbo-Gas M, Sanchis-Segura C, Carulli D,
976 Rossi F, Miquel M (2015a) The cerebellum on cocaine: plasticity and metaplasticity.
977 Addict Biol 20:941-955.

978 Vazquez-Sanroman D, Carbo-Gas M, Leto K, Cerezo-Garcia M, Gil-Miravet I, Sanchis-Segura
979 C, Carulli D, Rossi F, Miquel M (2015b) Cocaine-induced plasticity in the cerebellum of
980 sensitised mice. Psychopharmacology 232:4455-4467.

981 Vazquez-Sanroman DB, Monje RD, Bardo MT (2017) Nicotine self-administration remodels
982 perineuronal nets in ventral tegmental area and orbitofrontal cortex in adult male rats.
983 Addict Biol 22:1743-1755.

984 Vo T, Carulli D, Ehlert EM, Kwok JC, Dick G, Mecollari V, Moloney EB, Neufeld G, de Winter F,
985 Fawcett JW, Verhaagen J (2013) The chemorepulsive axon guidance protein
986 semaphorin3A is a constituent of perineuronal nets in the adult rodent brain. Mol Cell
987 Neurosci 56:186-200.

988 Wang D, Fawcett J (2012) The perineuronal net and the control of CNS plasticity. Cell and
989 tissue research 349:147-160.

990 Womelsdorf T, Schoffelen JM, Oostenveld R, Singer W, Desimone R, Engel AK, Fries P (2007)
991 Modulation of neuronal interactions through neuronal synchronization. Science
992 316:1609-1612.

993 Xue Y-X, Xue L-F, Liu J-F, He J, Deng J-H, Sun S-C, Han H-B, Luo Y-X, Xu L-Z, Wu P (2014)
994 Depletion of Perineuronal Nets in the Amygdala to Enhance the Erasure of Drug
995 Memories. The Journal of neuroscience 34:6647-6658.

996 Yamada J, Ohgomori T, Jinno S (2014) Perineuronal nets affect parvalbumin expression in
997 GABAergic neurons of the mouse hippocampus. The European journal of
998 neuroscience.

999

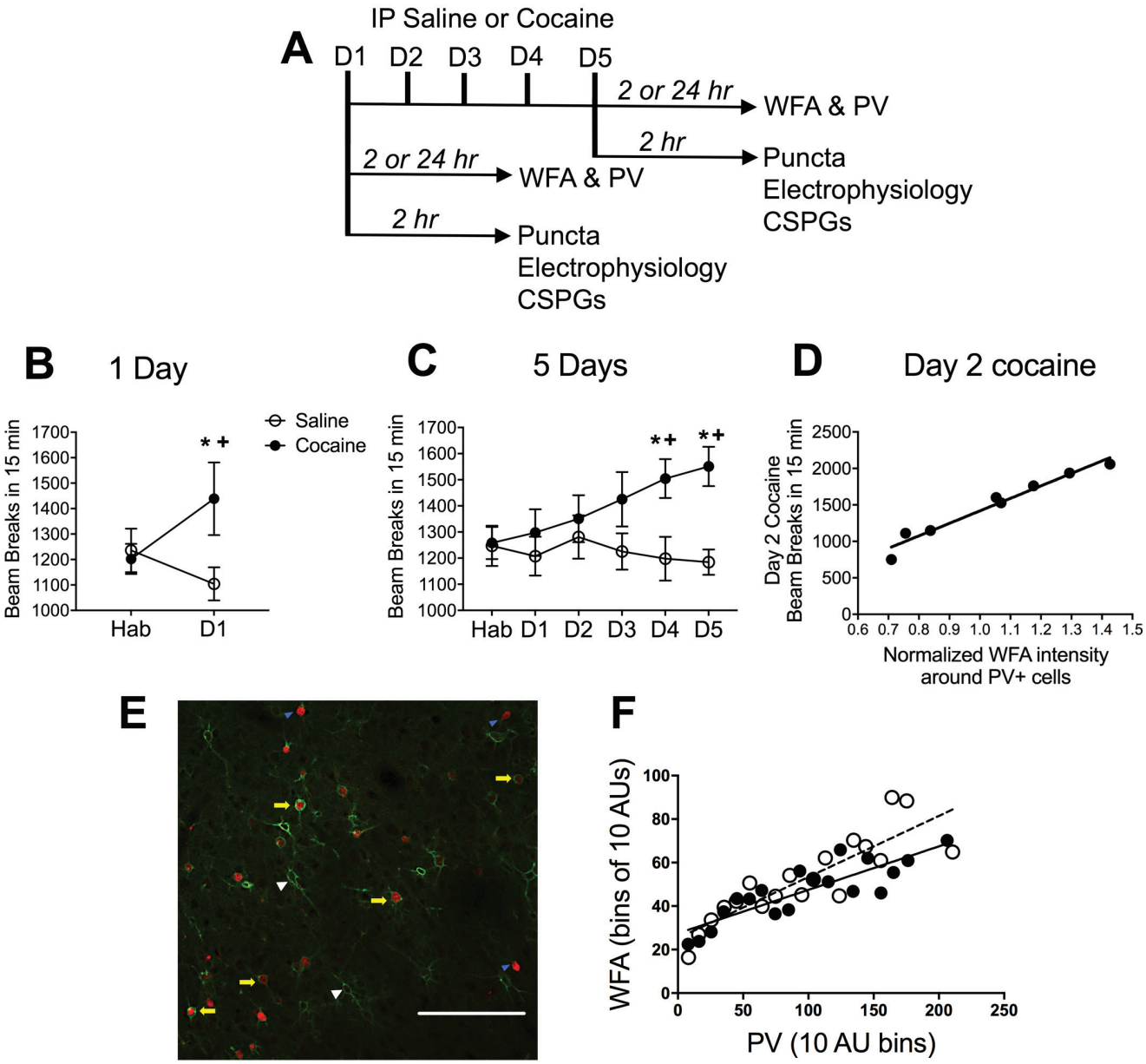


**Fig 1**

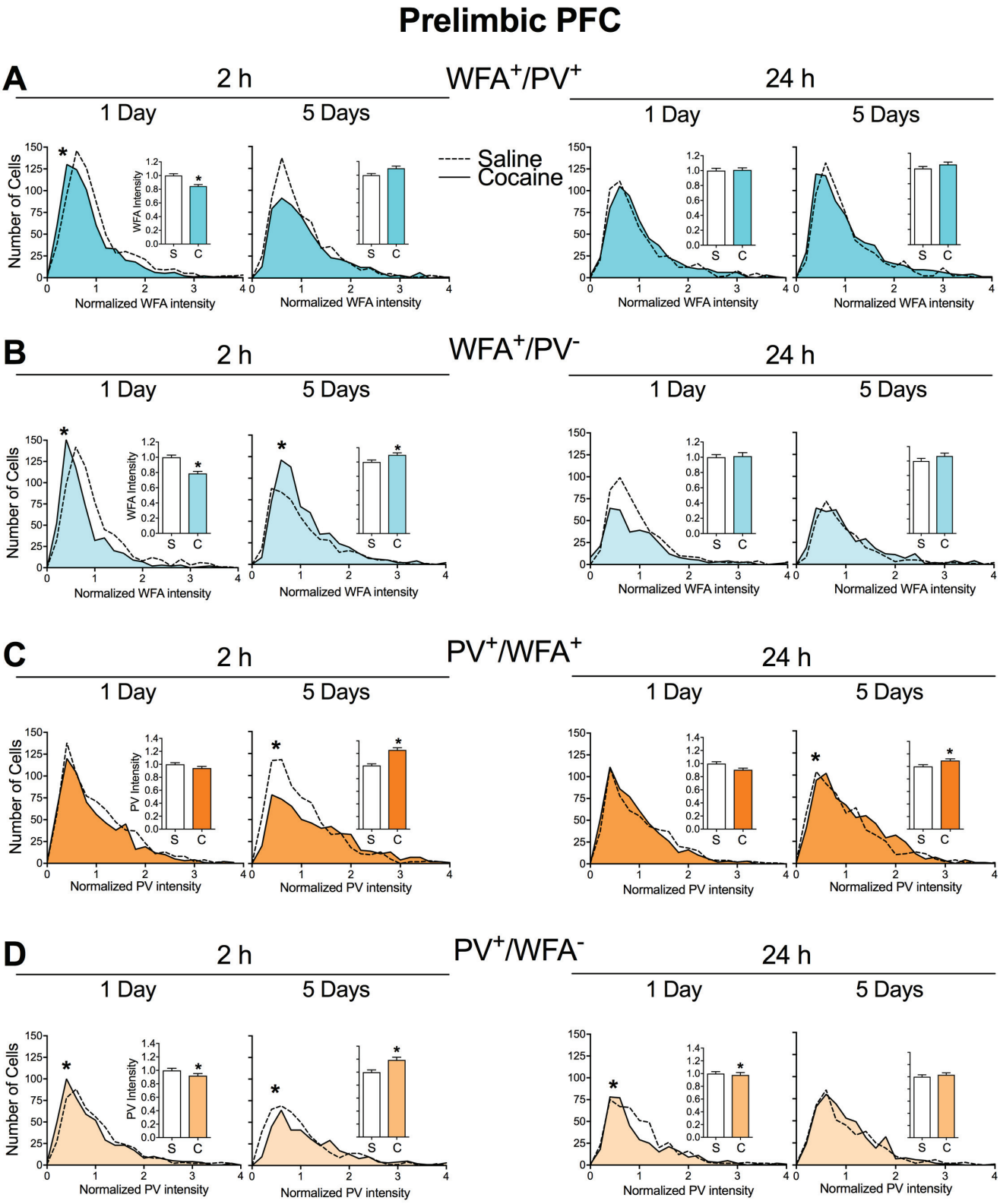


Fig 2

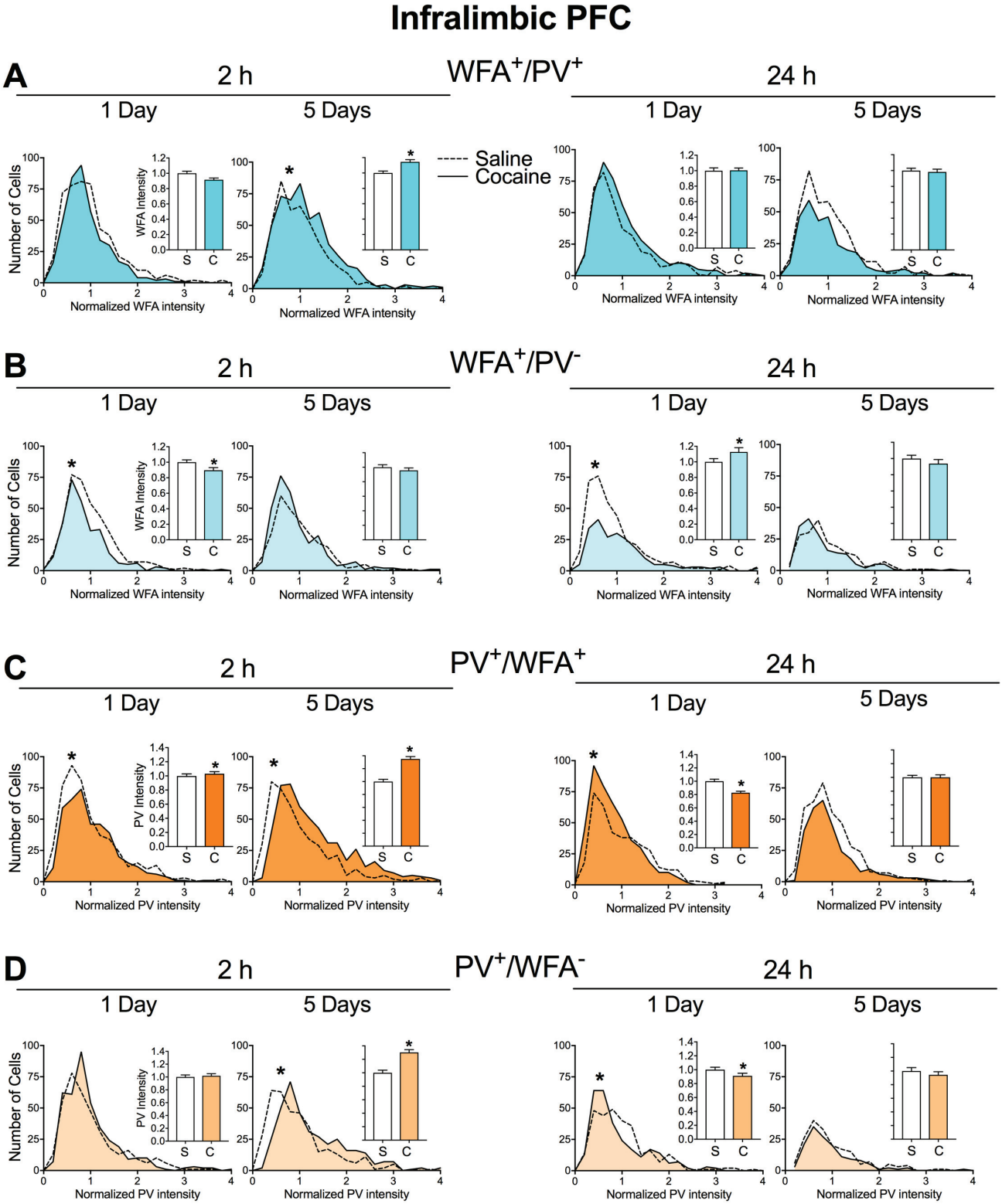


Fig 3

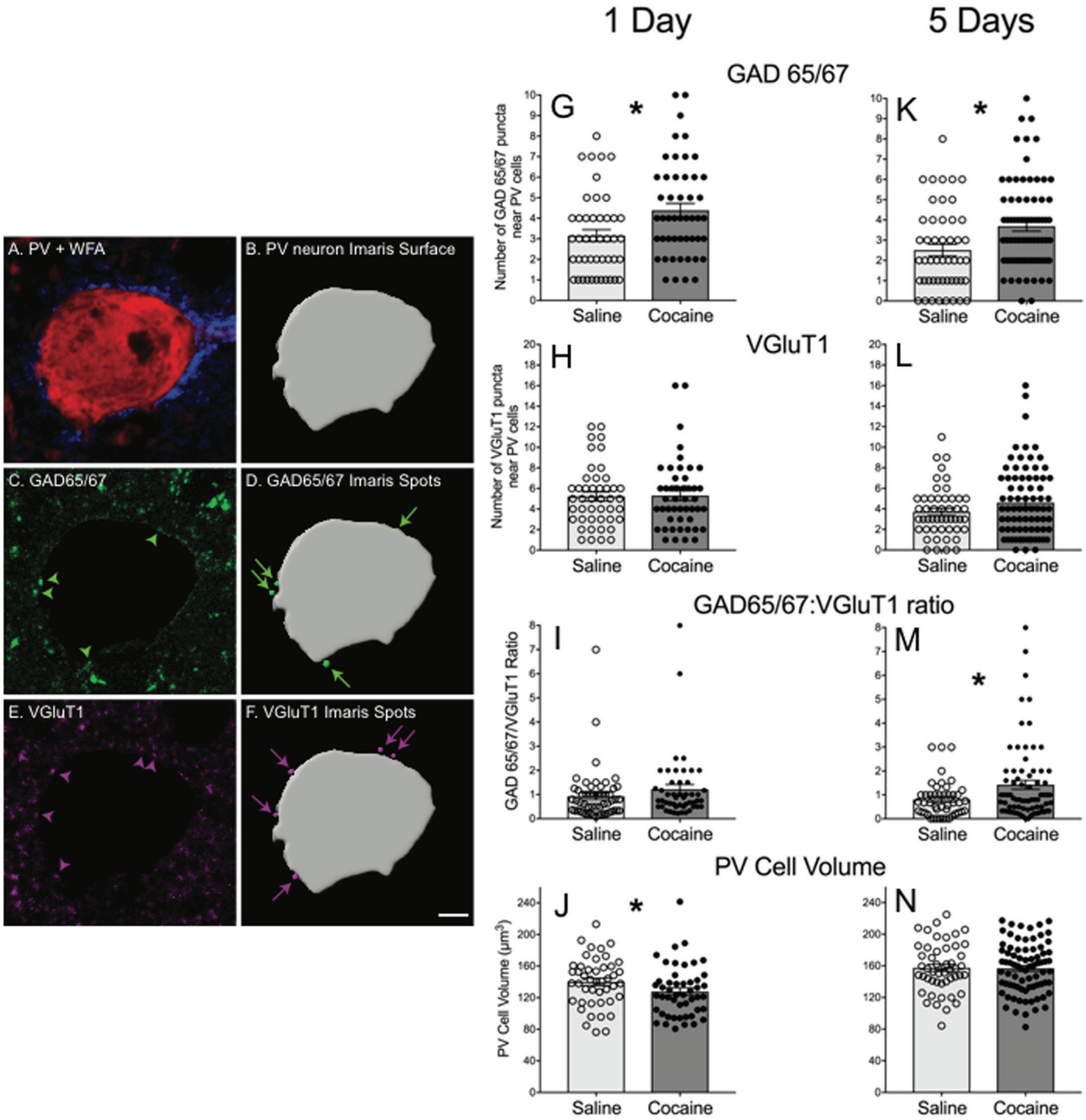


**Fig 4**

Figure 5

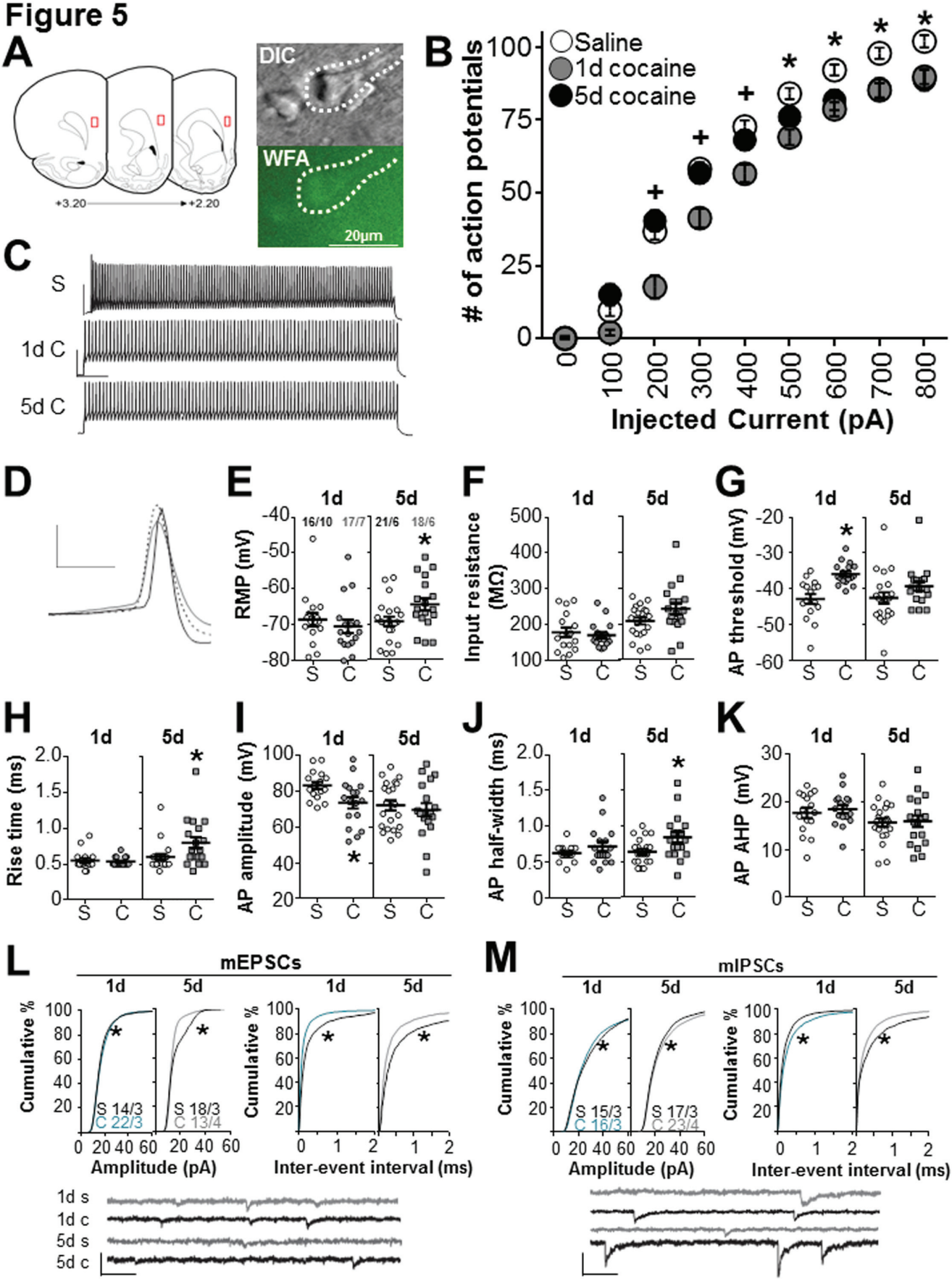

**Table 1.** Number of PV cells surrounded by WFA in prelimbic and infralimbic PFC after 1 day or 5 days of saline or cocaine

| Group | Drug | Region | $PV^+/WFA^+$ |
|---|---|---|---|
| 1 Day 2 h | Sal | Prelimbic | 88 ± 14 |
| | Coc | | 77 ± 8 |
| | Sal | Infralimbic | 61 ± 6 |
| | Coc | | 51 ± 7 |
| 5 Days 2 h | Sal | Prelimbic | 80 ± 12 |
| | Coc | | 70 ± 10 |
| | Sal | Infralimbic | 61 ± 8 |
| | Coc | | 66 ± 8 |
| 1 Day 24 h | Sal | Prelimbic | 89 ± 18 |
| | Coc | | 91 ± 21 |
| | Sal | Infralimbic | 45 ± 5 |
| | Coc | | 43 ± 11 |
| 5 Days 24 h | Sal | Prelimbic | 102 ± 16 |
| | Coc | | 108 ± 14 |
| | Sal | Infralimbic | 67 ± 8 |
| | Coc | | 49 ± 9 |

**Table 2.** Composition of GAGs in mPFC after 1 day or 5 days of saline or cocaine

| | Group | 1 Day | | 5 Days | |
|---|---|---|---|---|---|
| | | Saline | Cocaine | Saline | Cocaine |
| Total GAG Composition | HS | 17.9 ± 4.1% | 19.3 ± 6.9% | 18.4 ± 2.2% | 17.2 ± 2.7% |
| | CS | 54.3 ± 8.2 | 51.7 ± 11.6 | 52.8 ± 4.1 | 56.8 ± 4.4 |
| | HA | 27.8 ± 10.6 | 29.0 ± 13.6 | 28.8 ± 6.2 | 26.0 ± 6.9 |
| HS Composition | TriS | 2.3 ± 1.2% | 2.2 ± 1.6% | 1.6 ± 0.4% | 1.8 ± 0.2% |
| | NS6S | 4.4 ± 1.3% | 3.9 ± 1.8 | 3.9 ± 0.7 | 4.2 ± 0.6 |
| | NS2S | 11.9 ± 3.5% | 10.8 ± 4.1 | 8.7 ± 1.2 | 10.5 ± 0.8 |
| | NS | 17.8 ± 2.9 | 16.7 ± 4.8 | 17.7 ± 1.3 | 18.2 ± 1.1 |
| | 2S6S | 0.1 ± 0.1 | 0.2 ± 0.1 | 0.1 ± 0.1 | 0.1 ± 0.1 |
| | 6S | 2.7± 1.2 | 2.6 ± 1.3 | 2.8 ± 0.5 | 3.0 ± 0.3 |
| | 2S | 0.5 ± 0.1 | 0.3 ± 0.2 | 0.5 ± 0.1 | 0.4 ± 0.1 |
| | 0S | 60.4 ± 8.9 | 63.2 ± 12.4 | 64.6 ± 3.6 | 61.7± 2.7 |
| CS Composition | 2S4S | 0.2 ± 0.1% | 0.2 ± 0.1% | 0.2 ± 0.1% | 0.3 ± 0.1% |
| | 2S6S | 1.1 ± 0.5 | 1.0 ± 0.5 | 0.8 ± 0.3 | 1.0 ± 0.3 |
| | 4S6S | 1.1 ± 0.2 | 1.1 ± 0.3 | 0.9 ± 0.1 | 1.0 ± 0.1 |
| | 4S | 89.8 ± 3.9 | 89.5 ± 3.4 | 90.3 ± 1.5 | 89.1 ± 2.0 |
| | 6S | 2.4 ± 0.9 | 1.9 ± 0.8 | 2.2 ± 0.5 | 2.7 ± 0.9 |
| | 2S | 0.2 ± 0.1 | 0.1 ± 0.1 | 0.2 ± 0.1 | 0.1 ± 0.1 |
| | 0S | 5.2 ± 2.5 | 6.1 ± 3.7 | 5.3 ± 1.5 | 5.8 ± 0.9 |